

Performance of Continuous Hydrogen Production from Perhydro Benzyltoluene by Catalytic Distillation and Heat Integration Concepts with a Fuel Cell

Timo Rüde, Yulin Lu, Leon Anschütz, Marco Blasius, Moritz Wolf, Patrick Preuster, Peter Wasserscheid, and Michael Geißelbrecht*

The benzyltoluene-based liquid organic hydrogen carrier (LOHC) system enables the safe transport and loss-free storage of hydrogen. At least 26% of the lower heating value of the released hydrogen, however, has to be invested in form of heat to release the stored hydrogen. The low operation temperatures of catalytic distillation (CD) can facilitate waste heat integration to reduce external heat demand. Herein, the continuous hydrogen release from perhydro benzyltoluene via CD is demonstrated. It is revealed in the experimental results that this mode of operation leads to a high hydrogen release rate and very efficient noble metal catalyst usage at exceptionally mild conditions. The hydrogen-based productivity of platinum of $0.35 \text{ g}_{\text{H}_2} \text{ g}_{\text{Pt}}^{-1} \text{ min}^{-1}$ ($0.7 \text{ kW}_{\text{LHV, H}_2} \text{ g}_{\text{Pt}}^{-1}$) at a dehydrogenation temperature of only $267 \text{ }^\circ\text{C}$ is found to be nearly four times higher than for the conventional continuous liquid-phase dehydrogenation at the same temperature. Furthermore, simulation results of the CD process are described. The feasibility of a fully heat-integrated process for electricity generation from the released hydrogen via CD using waste heat from the fuel cell for the CD reboiler is demonstrated. The technical potential of coupling the H12–BT dehydrogenation by CD with high-temperature fuel cell operation is highlighted by the simulation.

systems consist of at least one hydrogen-lean and one hydrogen-rich molecule. Hydrogen is bound to the hydrogen-lean LOHC molecule via an exothermic hydrogenation reaction. In this LOHC-bound form, hydrogen can be stored safely at ambient conditions and without losses. Hydrogen recovery from the hydrogen-rich LOHC molecule is achieved by the reverse reaction, an endothermic dehydrogenation reaction. None of the components of the LOHC system are consumed in this cyclic storage process that builds on the multiple recycling (many hundred times) of the organic hydrogen carrier molecules.^[4] Additionally to benign ecotoxicology, the LOHC components should have a wide liquid range, especially down to $-30 \text{ }^\circ\text{C}$, to allow usage under cold climatic conditions.^[5–6]

The historical development of pure hydrocarbon LOHC systems has first considered the toluene-based LOHC system. This system, however, has the drawbacks


of a relatively low flashpoint, coke formation under the gas-phase dehydrogenation conditions, relatively low hydrogen purity due to the high volatility of the involved LOHC compounds, and considerable toxicity issues.^[7–8] The dibenzyltoluene-based LOHC system has a substantially lower volatility, which

1. Introduction

Liquid organic hydrogen carrier (LOHC) systems can be applied to store hydrogen over extended periods of time or to transport hydrogen using the existing fuel infrastructure.^[1–3] LOHC

T. Rüde, Y. Lu, L. Anschütz, P. Wasserscheid, M. Geißelbrecht
Lehrstuhl für Chemische Reaktionstechnik
Friedrich-Alexander-Universität Erlangen-Nürnberg
Egerlandstr. 3, 91058 Erlangen, Germany
E-mail: m.geisselbrecht@fz-juelich.de

T. Rüde, M. Blasius, P. Preuster, P. Wasserscheid, M. Geißelbrecht
Forschungszentrum Jülich
Helmholtz-Institute Erlangen-Nürnberg for Renewable Energy (IEK 11)
Egerlandstr. 3, 91058 Erlangen, Germany

 The ORCID identification number(s) for the author(s) of this article can be found under <https://doi.org/10.1002/ente.202201366>.

© 2022 The Authors. Energy Technology published by Wiley-VCH GmbH. This is an open access article under the terms of the Creative Commons Attribution License, which permits use, distribution and reproduction in any medium, provided the original work is properly cited.

DOI: 10.1002/ente.202201366

M. Wolf
Karlsruhe Institute of Technology
Engler-Bunte-Institute
Engler-Bunte-Ring 1, 76131 Karlsruhe, Germany

P. Preuster
Department Mechatronics and Mechanical Engineering
Bochum University of Applied Sciences
Am Hochschulcampus 1, D-44801 Bochum, Germany

P. Preuster
Fraunhofer IEG
Fraunhofer Research Institution for Energy Infrastructure and Geothermal Systems IEG
Am Hochschulcampus 1, D-44801 Bochum, Germany

led to remarkable progress in dehydrogenation catalyst development,^[9–11] since catalyst testing below the atmospheric boiling point is viable at high temperature. High-temperature dehydrogenation in the liquid phase is also feasible with the benzyltoluene-based LOHC system in technical reactors at raised pressure. Hereby hydrogen purification by condensation of evaporated LOHC components is more challenging but still efficiently achievable.^[7] Since the dibenzyltoluene-based LOHC system suffers from high viscosity of the hydrogen-rich H18-DBT at low temperatures^[5,7] benzyltoluene (H0-BT)/perhydro benzyltoluene (H12-BT) has gained significant interest as LOHC system in recent years.^[12–14] It has been demonstrated, for example, that the hydrogen release rate at identical pressure and temperature is higher for the dehydrogenation of H12-BT than for H18-DBT.^[12,15] Additionally, the high stability of the benzyltoluene-based LOHC system was demonstrated in several successive hydrogenation and dehydrogenation cycles with minimal byproduct formation.^[7]

Runge et al. evaluated the mobility costs of different renewable fuels produced at a time and place with excess renewable energy at different locations worldwide with subsequent transportation to Germany by ship and distribution via trucks.^[16] Hydrogen showed the lowest mobility costs for the five out of seven farther afield locations when distributed via the dibenzyltoluene-based LOHC system. The benzyltoluene-based LOHC system should perform slightly better considering the faster hydrogen release rate and the slightly lower hydrogen release enthalpy compared to the dibenzyltoluene-based LOHC system.^[5,7] A recent technoeconomical study showed that LOHCs outmatch compression, liquefaction or pipelines as a means for hydrogen transport especially over long distances.^[17] However, the study points out that for effective hydrogen transport via LOHC systems, waste heat integration should be considered to provide the required heat of dehydrogenation. Note that the technical dehydrogenation of methylcyclohexane to toluene and of H18-DBT to H0-DBT is typically operated at temperature levels of 350–400 °C^[18–21] and 300–340 °C,^[22–24] respectively. Lowering the dehydrogenation temperature reduces heat losses and enables easier integration of industrial waste heat sources.

For such heat integration, several options have been proposed. Heat integration for stationary applications between the exothermic hydrogen charging and the endothermic hydrogen discharging processes is possible, but can only be realized at the same location with efficient long-term heat storage.^[25] This is relevant for example in combination with the hot pressure swing reactor concept that enables both hydrogenation and dehydrogenation in the same apparatus.^[26,27] An alternative to provide the dehydrogenation enthalpy more location independent is to utilize the waste heat of a downstream process utilizing hydrogen, such as fuel cells,^[28] engines, and turbines which typically have an efficiency of 50% and less.^[29,30] Among the various types of fuel cells, SOFCs have been proposed due to their high exhaust gas level,^[31–33] but they typically suffer from limitations regarding their dynamic operability.^[3] Polymer electrolyte membrane (PEM) fuel cells can be operated dynamically and high-temperature PEM fuel cells (HT-PEM-FCs) were developed for increased temperature levels,^[34] for example, operation at 240 °C has been demonstrated.^[35,36] Thermal coupling of such

HT-PEM FCs with a hydrogen release unit with catalytic distillation (CD) therefore seems to be within reach.^[37]

Recently, we presented the concept (cf. Figure S1, Supporting Information) to lower the LOHC dehydrogenation temperature below 240 °C by employing CD in a batch-mode H12-BT dehydrogenation reaction.^[37] Note that the integration of a heterogeneously catalyzed reaction with distillation is the industrial forerunner in process-intensification methods^[38,39] and the term CD emphasizes that a heterogeneous catalytic process is employed, whereas in reactive distillation, a homogenous or heterogeneous catalyst could be used.^[39–43] The goal of our former work was to prove that CD can suppress product inhibition by enriching the more volatile H12-BT in the catalyst packing of a CD setup. The benzyltoluene-based LOHC system was applied for this study since the temperature window of the H12-BT/H0-BT distillative separation matches the temperature range of the dehydrogenation.^[40] The boiling points of the dibenzyltoluene-based LOHC system are too high to enable CD within the thermal stability limits of this organic carrier.^[44,45] The toluene-based LOHC system, in contrast, is impractical for the CD approach as the system would require high operation pressure due to its low boiling point.^[46] Note that the temperature and reaction pressure are coupled in CD where the dehydrogenation reaction proceeds at boiling conditions. Due to the boiling condition and the low hydrogen partial pressure as a consequence thereof, CD enables hydrogen release at very low temperature. The batch CD dehydrogenation of H12-BT was demonstrated at 202 °C, which is the lowest reported temperature of hydrogen release for a non-condensed, purely hydrocarbon LOHC system.^[37]

Herein, we advance the CD concept for the dehydrogenation of LOHC systems by first demonstrating hydrogen release from LOHC systems by CD in continuous operation with improved effectiveness of the separation section for enhancing the hydrogen production rate at mild conditions. Second, a process simulation based on the experimental CD data is utilized to study the effect of residence time and boil-up ratio (BR) on the performance.^[47] A further focus of this study is on the heat demand of the combined reaction and distillation process and we evaluate heat integration options between the CD process and a downstream operated fuel cell.

2. Experimental Section

2.1. Apparatus and Procedure

The applied experimental setup is similar to the apparatus used for conducting the batch experiments described in our previous paper and adapted to account for the continuous dehydrogenation concept (cf. Figure S1, Supporting Information).^[37] The CD setup for continuous release of hydrogen consisted of four parts: an evaporator, a separation section, a catalytic section, and a condenser. The separation and catalytic sections were enclosed in a glass column ($d = 30$ mm, $h = 450$ mm). The column was attached to a three-necked flask, which represented the bottom of the column. To reduce heat loss, the aforementioned flask and the connection were wrapped in glass wool. Liquid benzyltoluene with a given degree of dehydrogenation (Hx-BT) was fed from the bottom by a high performance liquid chromatography

(HPLC) dosing pump (WADose V3.4, Flusys GmbH) to the evaporator (DV4-S-1709-1, ADROP GmbH). Thereby, the reboiling vapor flow of Hx-BT at the bottom of the column was controlled precisely. Hydrogen gas was separated from the Hx-BT vapor at the top of the column by a total vapor condenser. The reliquified Hx-BT still had hydrogen stored in it and was therefore returned to the packed bed in the column whereby the reflux was established, leading to a circular countercurrent flow within the column. Additionally, raw H12-BT reactant was continuously fed into the top of the column, where the concentration of H12-BT was highest. This is a general recommendation for the design of CD although in principle H12-BT can be fed anywhere into the reaction section. Continuous Hx-BT product removal from the bottom flask was realized via a peristaltic pump. The glass column was wrapped in a temperature controlled (HT MC1, Horst GmbH) electric heat jacket (HJ) to reduce heat losses to the substantially colder surrounding. The aim is to achieve an adiabatic column with heat provision for the whole process solely by the reboiler.^[48] Distillation columns, however, are not isothermal in general^[49] and in the presented laboratory setup an imperfect insulation in combination with a nonuniform tempered heating jacket may entail heat losses as well as unintended heat input.

The separation section, which was located in the lower part of the column, was filled with glass Raschig rings (6×6 mm). According to literature, glass Raschig rings can achieve one theoretical separation stage every 50–140 mm of packing height.^[50] Our own separation experiments with H12-BT and H0-BT mixtures were carried out at reduced absolute pressures and with total reflux. The 400 mm high packing in the separation experiments could achieve an increase in molar fraction of H12-BT from bottom to top of 34–45% points.

H12-BT had a lower atmospheric boiling point than H0-BT ($\text{bp}(\text{H12-BT}) = 270^\circ\text{C}^{[12]}$ vs. $\text{bp}(\text{H0-BT}) = 282^\circ\text{C}^{[51]}$). Therefore, H12-BT enriched in the upper part, while H0-BT accumulated in the lower part of the separation section.^[12] The catalytic section was placed above the separation section to exploit the higher concentration of H12-BT. Commercial spherical catalyst pellets with an average diameter of 2.8 mm (Clariant, EleMax-D101)^[52] were placed in the reaction section. The catalyst pellets consisted of an alumina support and an eggshell-like layer of platinum nanoparticles with a total noble metal loading of 0.3 wt%.^[11] A tubular wire mesh ($d = 10$ mm) was inserted in the center of the radius of the upper part of the column. The wire mesh formed a gas channel to increase the available void area since flooding was a major issue in any countercurrent operation especially with catalytic internals.^[43] Note that the catalytic internals clearly offer further development potential^[53,54] which we have addressed^[51] but will be described in more detail separately. This publication focuses on operational aspects of the CD with a technically established catalyst to allow for comparability with existing processes and literature. The temperature profile of the column was measured with a five-point thermocouple that was introduced via the column head. The separation of hydrogen gas and Hx-BT vapor in the reflux condenser was realized with a borosilicate glass Dimroth condenser and cooling water. Downstream, the condenser was connected to a hydrogen thermal mass flow meter (MFM) to monitor the released hydrogen flow. The pressure was monitored at the

condenser by a digital manometer. **Figure 1A** shows a scheme of the applied CD setup for continuous dehydrogenation of H12-BT.

During preparation of the experiment, a defined amount of glass Raschig rings (6×6 mm) was filled into the column and the catalyst pellets were placed on top. H12-BT was added to the three-necked flask, which was connected to the column at the bottom. The liquid-level of H12-BT was chosen in a way that the pipes leading to the evaporator and the discharge of the hydrogen-lean Hx-BT were always hydrostatically at a lower level. Afterward, the setup was flushed with argon for 10 min to remove residual air from the setup. The evaporator was heated and after reaching its set temperature, the HPLC dosing pump was started. Parallel, the temperature in the heating jacket of the column was increased to the selected reaction temperature. After reaching the target temperature, the peristaltic pumps were started to ensure feed and product flow. The steady-state was reached, when the hydrogen flow detected by the MFM remained constant for at least 30 min.

A description of the setup for liquid-phase dehydrogenation of H18-DBT is provided in the supporting information.

2.2. Mathematical Model

In this section, the applied mathematical models are introduced. Four different approaches can be distinguished for modeling a CD. The approach can be based on the assumption of vapor–liquid (thermal, physical) phase equilibrium (EQ) or rate-based mass transfer (non-equilibrium stage) between the vapor and liquid phases (NEQ).^[55] Both EQ and NEQ can be combined with either a chemical reaction equilibrium model or a kinetic approach for the reaction.^[56] Even though it is proposed that NEQ models should be routinely employed,^[57] EQ models are popular in literature.^[58] In addition to thermodynamic properties, NEQ models require physical properties such as surface tension, diffusion coefficients, viscosities, etc., for calculation of mass (and heat) transfer coefficients and interfacial areas.^[55] By assuming equilibrium stages, no further details are required for heat- and mass-transfer correlations for the specific type of packing.^[59] This allows for quick estimations of distillation column sizing with experimental, literature, or manufacturer height equivalent to one theoretical plate (HETP) values of various laboratory distillation packings.^[50] Furthermore, Sundmacher argues that for heterogeneously catalyzed CD processes, NEQ is only worthwhile for very fast reactions, since determining the necessary mass transfer parameters is usually very time-consuming.^[60] The reaction by contrast is often modeled with a kinetic equation to investigate influencing factors such as residence time and temperature/pressure.^[58] Since heat and mass transfer properties for the benzyltoluene-based LOHC system are not fully available and the LOHC dehydrogenation has a low driving force under the applied conditions and hence is rather slow, an EQ model containing a rate expression for the chemical reaction is developed in this paper. In future, the model can be enhanced by including more details regarding heat and mass transfer.

The vapor–liquid equilibrium is calculated by the predictive γ -model UNIFAC-Dortmund, which is based on group contributions and frequently used for mixtures without available vapor–

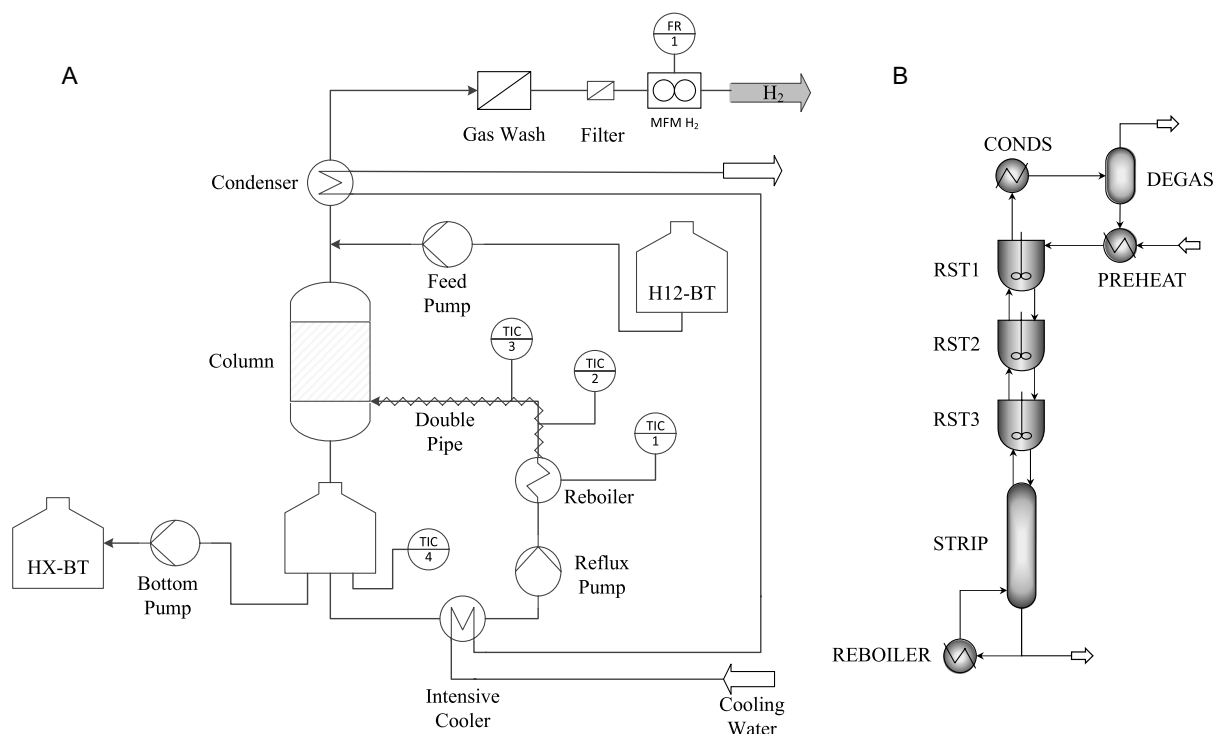


Figure 1. Process flow sheets: A) experimental setup of continuous H12-BT dehydrogenation in a catalytic distillation (CD) column; B) simulation flow sheet with three catalytic stages.

liquid equilibrium (VLE) measurements because of its simple inputs but reliable estimates.^[61–64] UNIFAC-Dortmund compared to UNIFAC adds group parameters of cyclic alkyl groups and extends the applicable temperature range^[65] up to 180 °C for alkanes and aromatics by introducing temperature-dependent group-interaction parameters.^[63] The lack of experimental data above 180 °C makes extrapolation for the LOHC dehydrogenation necessary. To apply UNIFAC-Dortmund, the respective molecule is divided into functional groups that are included in the database.^[66] For the calculation of the VLE, vapor pressure data in the form of Antoine coefficients are utilized. Many vapor pressure data sets and boiling point measurements are available in literature, which in some cases differ distinctly from each other.^[7] For consistency reasons, the coefficients we used were derived from measurements of isomeric mixtures of H0-BT and H12-BT in experiments conducted in the same setup by the same procedure.^[51]

The heterogeneously catalyzed LOHC dehydrogenation is a highly complex three-phase reaction. Heterogeneously catalyzed reactions comprise several steps that include—in addition to the surface reaction step—film and pore diffusion as well as adsorption and desorption steps.^[67] Which and how many of the steps are considered in a suitable model depends on the question whether one step can unambiguously be identified as the rate determining step.^[68] The hydrogen gas formation in the catalyst pellets can provide a strong convective mass transfer component. Moreover, the formation of hydrogen bubbles within a catalyst pore network can lead to an oscillatory motion.^[69,70] For the case of hydrogen release from LOHC systems by dehydrogenation, it

has been shown that the reaction rate in a state where oscillatory hydrogen bubble nucleation takes place can be up to 50 times higher than a nucleation inhibited state of the same catalyst under otherwise identical conditions.^[71] Moreover, the liquid holdup can influence the residence time in the catalytic section.^[72,73] It is noteworthy that the reaction takes place primarily in the liquid phase, since the catalyst pellets must be wetted to maintain distillation premises.^[40,74] The liquid holdup is subject to the conditions of the vapor–liquid countercurrent flow in the fixed bed for which some empirical models are given in the literature.^[75] computational fluid dynamics (CFD) simulations may prove useful for this purpose in the future.^[76,77]

To effectively study the reaction behavior of the LOHC dehydrogenation, we choose to utilize batch CD experimental data^[37] and fit them to a power law-based kinetic model. The data are slightly influenced by the separation section in the experiment. However, the complex phenomena discussed before are implicitly included in this model. Previously, LOHC dehydrogenation experiments have been represented adequately by power law models. Usually, only one reaction step and no backward reaction were assumed if the kinetics of LOHC dehydrogenation reactions were described far from the equilibrium.^[78,79] Mrusek successfully extended a power law model to include the impairment of the reaction rate with decreasing driving force when the reaction approached the chemical equilibrium.^[80] In the case of the CD process the hydrogen partial pressure is artificially lowered due to the boiling condition of the organic carrier.^[37] This increases the thermodynamic driving force for the dehydrogenation considerably.^[7,37] Therefore, in this study,

we fit the experimental degree of dehydrogenation over time (DoDH-over-t) data at various pressures obtained from a former study^[37] by utilizing the power law kinetic Equation (1). The kinetic parameters (κ_0 , E_A , n) are fitted with a least squares objective function and the python library `scipy.optimize.minimize`.^[81]

$$\begin{aligned} \frac{d\text{DoDH}}{dt} \left[\frac{1}{s} \right] &= - \frac{\kappa_0 \left[\frac{1}{L^3} \right] \cdot m_{\text{cat}} \left[\frac{g}{L} \right]}{\rho_{\text{bulk}} \left[\frac{g}{L} \right]} \cdot \exp \left(- \frac{E_A \left[\frac{kJ}{\text{mol}} \right]}{RT} \right) (1 - \text{DoDH} [-])^n \\ &= - \frac{18290.7 \left[\frac{\text{mol}^{1-0.929}}{L^{1-0.929} \cdot s} \right] \cdot m_{\text{cat}} \left[\frac{g}{L} \right]}{550 \left[\frac{g}{L} \right]} \cdot \exp \left(- \frac{67.6 \left[\frac{kJ}{\text{mol}} \right]}{RT} \right) (1 - \text{DoDH} [-])^{0.929} \end{aligned} \quad (1)$$

Specifications of the reactor model such as the bulk volume of the catalytic section can then be calculated by including the catalyst packed bulk density $\rho_{\text{bulk}} = 550 \text{ g L}^{-1}$ provided by the manufacturer.^[82] We assume that hydrogen release occurs from liquid LOHC and therefore the concentration of H12-BT in the liquid phase can serve as the driving force and input for Aspen Plus. The initial concentration of H12-BT $c_{\text{H12-BT},0}$ is given as the ratio of the liquid density of H12-BT to the molar mass of H12-BT. It is assumed that the concentration of H12-BT decreases only due to the decreasing amount of H12-BT in the liquid phase.

The overall CD model is developed with the described VLE and kinetic models in the commercial simulation software Aspen Plus to resemble the experimental setup described earlier. Therefore, the CD is divided into a stripping section and a catalytic section (see Figure 1B). Since in the experimental setup, the column is wrapped in a heating jacket to compensate for heat loss to the surrounding, the simulation assumes an adiabatic CD. The sole enthalpy source for the CD is the reboiler. The stripping section is simulated by the RadFrac model with a kettle reboiler to introduce heat directly to the liquid at the bottom of the column leading to vaporization.

The catalytic stages are modeled as biphasic continuous stirred tank reactor (CSTR). Own experiments in the same column with lighter (*n*-tetradecane, bp = 252–254 °C)^[83] and heavier boiling (*n*-hexadecane, bp = 285–287 °C)^[84] unreactive tracers revealed Bodenstein numbers of about 0.24 indicating strong backmixing and deviation from plug flow in our system.^[67,68] This is within literature values that suggest strong axial dispersion in CD systems is not unlikely^[85] with Peclet numbers lower than 10^[86,87] or even Peclet^[41] and Bodenstein^[54] numbers below 0.1.^[54] In the simulation, we set the number of CSTRs to be 3 to avoid a very complicated flow sheet but to allow for studying slight changes in intermediate variables like reaction rate and

concentration from one catalytic stage to another. The simulation studies retrospectively indicate that assuming strong backmixing is suitable and only mild changes of concentration and temperature are observed from one CSTR to another. On each discretized catalytic stage, the kinetic and MESH equations for the material (MB) and energy balance (HB) must be solved together to obtain reaction rate and stream flows (Figure 2). For all stages, the phase equilibrium links the variables T , p , x , and γ firmly together.^[88] By modeling three separate CSTRs, intermediate variables like reaction rate and concentration on each catalytic stage can be analyzed directly.

2.3. Performance Indicators

The hydrogen production rate in the experiments can be calculated from liquid samples by determining the degree of dehydrogenation (DoDH), by refractometry or by gas chromatography.^[89,90] The details for the determination of DoDH via refractive index^[91] have been adapted to the H12-BT/ H0-BT LOHC-system and the calibration curve, and can be found in Supporting Information. The DoDH is defined as the ratio of reversibly released hydrogen to the maximum amount of reversibly bound hydrogen in the LOHC. Thus, the DoDH can be seen as the conversion X of H12-BT or the yield Y of the hydrogen release assuming 100% selectivity due to very low by-product formation.^[7] At a DoDH of 100%, all H12-BT is converted to H0-BT and no reversibly bound hydrogen is left in the LOHC system, while the LOHC system is completely loaded with hydrogen at a DoDH of 0%.

The productivity P indicates the effectiveness of the catalytic section. P is defined as the total mass flow of H₂ released per mass of the active metal platinum and can be used to compare different experimental setups, for example, with different catalyst masses. Note that the productivity depends on the DoDH since the hydrogen release rate is dependent on the concentration of hydrogen-rich LOHC molecules.^[9,92] Under steady-state conditions, both the hydrogen release measured by the MFM and calculated from liquid-phase analyses of the feed and bottom streams are the same. The productivity at a specific DoDH can be calculated by dividing the mass flow of hydrogen \dot{m}_{H_2} by the mass of noble metal in the experimental setup m_{nm} according to Equation (2).

$$P_{\text{DoDH}} = \frac{\dot{m}_{\text{H}_2}}{m_{\text{nm}}} \quad (2)$$

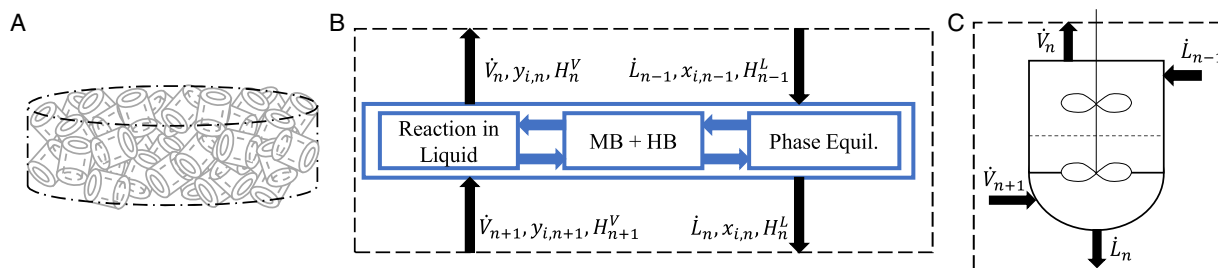


Figure 2. A) Discretization of one catalytic section in the CD column; B) important boundary conditions and key equations of the n th discretized catalytic stage; C) CSTR model of the n th catalytic stage.

3. Results and Discussion

3.1. Introduction of a Separation Section to the Continuous Dehydrogenation of H12–BT

To demonstrate the advantage of the separation section, we first conducted startup and continuous operation experiments at ambient pressure with and without separation section (cf. Figure S3, Supporting Information). In **Figure 3**, the released hydrogen flow and the stability of hydrogen release are shown with and without separation section in the continuous H12–BT dehydrogenation.

A maximum hydrogen volume flow of approximately 325 Nml min⁻¹ was obtained in both setups after an initial heating period of 40 min. In the setup with separation section, the hydrogen flow declined slightly over time during startup since pure H12–BT placed in the column bottom before startup did not match continuous stationary conditions. After 200 min, stationary continuous operation is reached at 280 Nml min⁻¹. In contrast, the flow of released hydrogen decreased strongly in the setup without separation section reaching a value of 210 Nml min⁻¹ after 160 min time-on-stream (TOS) without reaching stationary continuous operation.

The higher hydrogen release rate in the setup with separation section compared to the one without is mainly due to the increased concentration of H12–BT at the catalyst.^[37] Since the reboiler flask at the bottom is filled with pure H12–BT in the beginning of the experiment, similar initial H12–BT concentrations are expected at the catalyst. However, the amount of H12–BT decreases during the ongoing reaction and, consequently, the hydrogen release rate drops. Without separation section this effect is more pronounced as the separation section ensures a higher concentration of the lighter H12–BT at the catalyst. More H12–BT reactant in the catalyst bed kinetically promotes hydrogen release according to the power law kinetic equation for the CD (cf. nonzero reaction order according to Equation (1)). Additionally, the reduction of H0–BT at the catalyst

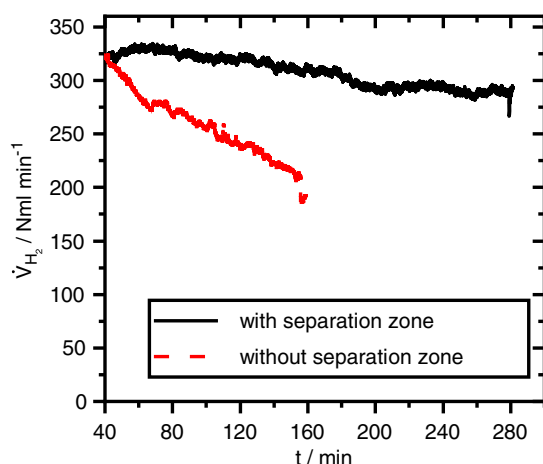


Figure 3. Comparison of the continuous H12–BT dehydrogenation with and without a separation section ($\dot{V}_{\text{evap}} = 15 \text{ mL min}^{-1}$, $T_{\text{evap}} = 300 \text{ }^\circ\text{C}$, $T_{\text{HJ}} = 280 \text{ }^\circ\text{C}$, $p = \text{atm}$, $\dot{m}_{\text{H12-BT}} = 0.8 \text{ g min}^{-1}$, catalyst 0.3 wt% Pt/Al₂O₃, $m_{\text{catalyst}} = 30.1 \text{ g}$, $m_{\text{packing}} = 106.0 \text{ g}$ or 11.0 g).

reduces product inhibition of the catalyst.^[37] Overall, the separation section enables higher hydrogen release rates after initial startup throughout the whole experiment.

After the initial decrease in hydrogen release rate (from 200 min TOS onward), the separation section shows a stable hydrogen release rate and steady-state operation. The measured hydrogen release rate of 280 Nml min⁻¹ (as detected by the MFM) corresponds well with the hydrogen release rate calculated from the difference in DoDH of the analyzed Hx-BT. Liquid sampling and gas chromatography of the feed (98% hydrogen loading, i.e., 2% DoDH) and the bottom streams (50% DoDH) in the steady-state result with the applied LOHC feed rate of 0.8 g min⁻¹ in an approximate hydrogen release rate of 265 Nml min⁻¹.

The temperature profile obtained by the five-point thermocouple indicates a slight decrease of temperature toward the top of the column (Figure S4, Supporting Information). Due to boiling condition and the vapor–liquid equilibrium the pressure and temperature as well as the composition in both phases are all linked together. The recently published vapor–liquid equilibrium data of the H12–BT/ H0–BT system states H12–BT as the light-boiler and H0–BT as the heavy-boiler.^[37] H12–BT therefore enriches toward the top of the column. To confirm this, liquid samples were collected during continuous operation of the CD setup (cf. Figure 1A) at the top of the reaction section and at the bottom of the column from the product discharge. As expected, with an atmospheric relative volatility of 1.3 assuming an equimolar binary mixture, the top samples consistently showed lower DoDH than the bottom samples. Nonetheless, the separation task with a difference in atmospheric boiling points of H12-BT and H0-BT of only about 12 K is challenging. The distillation task difficulty is comparable to methylcyclohexane toluene separation.^[46]

3.2. Productivity Dependence on Catalyst Bed Height

In a next set of experiments, the catalyst mass in the reaction section was reduced to assess its impact on the Pt-based productivity. Note that a fair comparison of the productivity is only possible for a similar DoDH of the product stream as the hydrogen release rate depends on the actual concentration of H12–BT. Therefore, the feed mass flow was adapted to obtain similar DoDHs for the different amounts of catalyst applied. The comparison of the Pt-based productivities for catalyst masses of 30.10 and 15.05 g in the reactor is shown in **Figure 4**.

In fact, the Pt-based productivity was found to be almost independent of the amount of the catalyst under given experimental variations. This indicates that the catalyst bed is well backmixed and operates at similar reactant concentrations for both catalyst amounts. A slight reduction in distillation section height to incorporate more catalyst does not compromise the space–time yield of the experimental setup. Consequently, hydrogen release per reactor volume can be increased without compromising platinum utilization. However, replacing distillation packing with catalyst can only be done to certain limits. Also, the height of the catalytic section in the evaluated range, which may influence hydrodynamics and the separation section, has little effect. Thus, the catalyst mass in the system can in general be further

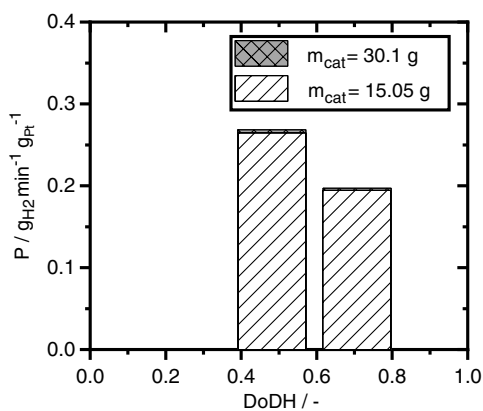


Figure 4. Dependency of the Pt-based productivity on the amount of catalyst ($\dot{V}_{\text{evap}} = 15 \text{ mL min}^{-1}$, $T_{\text{evap}} = 300 \text{ }^\circ\text{C}$, $T_{\text{HJ}} = 280 \text{ }^\circ\text{C}$, catalyst 0.3 wt% Pt/ Al_2O_3).

increased to enhance the volumetric power output of the CD dehydrogenation reaction.

3.3. Experimental Comparison of Continuous CD with Liquid-Phase Dehydrogenation

The following experiments target a comparison of the productivity in continuous CD compared to the more traditional operation mode of continuous liquid-phase dehydrogenation. This comparison is challenging since a liquid-phase dehydrogenation of H12-BT is not possible under the same temperature and pressure conditions as in the CD experiment. The high vapor pressure of the Hx-BT components under CD conditions does not allow a standard liquid-phase reaction. Note that the reaction pressure is directly linked to the temperature in the reaction section during CD.

To make the targeted comparison as fair as possible, we decided to juxtapose the CD of H12-BT and the liquid-phase dehydrogenation of H18-DBT. The chemical nature of H18-DBT is closely related to H12-BT, but the additional cyclohexyl group in the molecule leads to an elevated boiling point ($270 \text{ }^\circ\text{C}$ for H12-BT compared to $370 \text{ }^\circ\text{C}$ for H18-DBT). Since H18-DBT has a significantly lower vapor pressure, liquid-phase dehydrogenation is possible at the same temperature and absolute pressure conditions as applied in the CD setup with H12-BT. The comparison of productivities of the liquid-phase dehydrogenation of H18-DBT and the CD of H12-BT at an average catalyst temperature of $267 \text{ }^\circ\text{C}$ and at ambient pressure is shown in **Figure 5**. For both setups, the productivities decrease with increasing DoDHs. As already discussed, a lower concentration of hydrogen-rich LOHC and a higher concentration of inhibiting H0-LOHC product at the active catalyst reduce the hydrogen release rate.

The productivity of both experiments at a DoDH of 30% reveals a nearly four times higher value for the continuous hydrogen release in the CD setup compared to the liquid-phase dehydrogenation. At the applied, relatively mild reaction temperature of $267 \text{ }^\circ\text{C}$, the obtained productivity of $0.351 \text{ g}_{H_2} \text{ g}_{Pt}^{-1} \text{ min}^{-1}$ in CD is remarkably high. It compares to $0.095 \text{ g}_{H_2} \text{ g}_{Pt}^{-1} \text{ min}^{-1}$ in

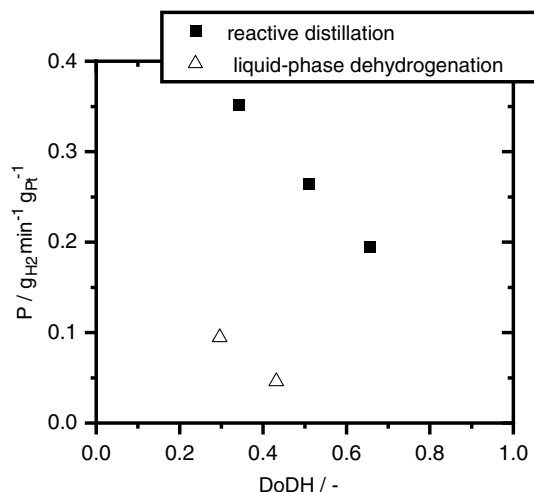


Figure 5. Comparison of the productivity in CD dehydrogenation of H12-BT and the liquid-phase dehydrogenation of H18-DBT with gas-liquid concurrent upstream at a catalyst temperature of $267 \text{ }^\circ\text{C}$ (CD: $\dot{m}_{\text{H12-BT}} = 0.22$ resp. 0.39 g min^{-1} , $\dot{V}_{\text{evap}} = 15 \text{ mL min}^{-1}$, $T_{\text{evap}} = 300 \text{ }^\circ\text{C}$, $T_{\text{HJ}} = 280 \text{ }^\circ\text{C}$, $p = 980 \text{ mbar}_{\text{abs}}$, catalyst 0.3 wt% Pt/ Al_2O_3 , $m_{\text{catalyst}} = 15.05 \text{ g}$, $m_{\text{packings}} = 126.6 \text{ g}$; liquid-phase dehydrogenation: $\dot{m}_{\text{H18-DBT}} = 0.23$ resp. 0.68 g min^{-1} , catalyst 0.3 wt% Pt/ Al_2O_3 , $m_{\text{catalyst}} = 44.3 \text{ g}$, $p = 980 \text{ mbar}_{\text{abs}}$).

the liquid-phase dehydrogenation of H18-DBT. At a DoDH of 40%, the extrapolated productivity difference is even more distinct with a nearly sixfold higher productivity for the CD process ($0.3 \text{ g}_{H_2} \text{ g}_{Pt}^{-1} \text{ min}^{-1}$ vs. $0.05 \text{ g}_{H_2} \text{ g}_{Pt}^{-1} \text{ min}^{-1}$). Note that in conventional liquid-phase dehydrogenation at $290 \text{ }^\circ\text{C}$, H_2 production from H12-BT at about $0.8 \text{ g}_{H_2} \text{ g}_{Pt}^{-1} \text{ min}^{-1}$ is only 30% faster than from H18-DBT.^[7] At $260 \text{ }^\circ\text{C}$ and ambient pressure, the productivity in the batch-dehydrogenation of H12-BT is also higher than for H18-DBT, but only threefold^[12] indicating a significant additional positive effect of the CD mode on the dehydrogenation rate. Note also that no signs of catalyst deactivation were observed during the herein applied relatively short reaction times. We anticipate, however, that catalyst deactivation by coke deposition, as described in the literature for gas-phase cycloalkane dehydrogenation,^[93] is in general much less pronounced in our gas/liquid-phase and pure liquid-phase dehydrogenation reaction. The hot liquid LOHC ensures a continuous hot wash of the catalyst material and, thereby, traces of high-boilers and coke precursors are continuously washed off the catalyst. These are indeed found as high-boiling compounds in the used LOHC material.

3.4. Validation of the Simulation with the Continuous Experiments

Our simulation targets the mathematical description of the steady-state performance of the CD dehydrogenation reaction. It stands to note that more than one steady-state could occur in CD due to the complexity of the coupled processes and strongly nonlinear behavior of the underlying models.^[94] The initial conditions are therefore decisive for the obtained simulation results, and they must be checked for plausibility especially

when using the simulation for optimizations or sensitivity studies. The equation-oriented (EO) method in Aspen is used, in which all models are solved simultaneously instead of working through the unit operations along the flow-direction according to sequential modular (SM) method. Also, loops are already included in EO as part of the connectivity equations. Therefore, they do not interfere with the convergence.^[95,96] Still, one SM simulation must be executed at the beginning to provide the initial values for the EO mode. After setting up the CD simulation for the LOHC dehydrogenation with the chosen models for reaction and distillation, the simulation was executed and it converged.

To benchmark the CD simulation with the experiment, the dependence of the DoDH on the feed rate for experiment and simulation is compared. The steady-state hydrogen release experimentally is determined indicating a significant additional positive effect of the CD mode on the dehydrogenation for three different reactant feed rates (0.2, 0.4, and 0.8 g min⁻¹) and a catalyst weight of $m_{\text{cat}} = 30$ g. These inputs in the simulation are set to match the experiment. The reboiler duty for the simulation is given based on the flow rate to the reboiler in the experiment assuming full evaporation of this stream. Thereby, the power consumption of the kettle reboiler was fixed to 42 W.

Figure 6 shows that the simulated DoDH is in the same range as the found experimental data. The trend of decreasing DoDH with increasing feed rate is also outlined. With increasing mass flow rate of H12–BT, the average residence time in the reactor decreases which leads to reduced DoDH. In the experiment, halving the reactant flow from 0.8 to 0.4 g min⁻¹ results in a 25% reduction in the hydrogen release and halving the reactant flow again to 0.2 g min⁻¹ results in a further 25% reduction in the hydrogen release. However, at larger feed rates, simulation and experiment deviate increasingly. At the feed rate of 0.8 g min⁻¹, the obtained DoDH is 56% higher in the experiment compared to the simulation. On the one hand, the assumption of 3 CSTRs might become less adequate at lower feed rates with lower back mixing. On the other hand, due to the fixed reboiler duty in all three experiments and simulations, the ratio of generated vapor to falling liquid decreases alongside with a growing

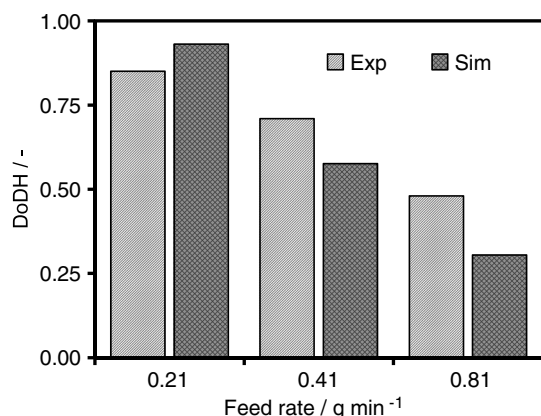


Figure 6. Performance comparison of the CD column with different feed rates (catalyst 0.3 wt% Pt/Al₂O₃, $m_{\text{catalyst}} = 30$ g, $\text{DoDH}_{\text{Feed}} = 1\%$, $\dot{V}_{\text{evap}} = 15$ mL min⁻¹, $p = \text{atm}$, $T_{\text{Feed}} = 30$ °C, $T_{\text{evap}} = 300$ °C, $\dot{Q}_{\text{evap}} = 42$ W).

liquid feed rate. This can cause insufficient heat provision to the catalytic section where the temperature decreases and limits the reaction rate in the simulation. Therefore, at higher feed rates, the whole temperature profile shifts to lower temperatures and the obtained release rates are lower. In the experiment, the heating jacket—originally intended to insulate the column and set to maintain a similar temperature on the column outside as inside—may act as an additional heat source, especially when the columns internal temperature drops. This may lead to a higher reaction rate and DoDH for high feed rates in the experiment. Furthermore, the comparison of simulation and experiment indicates possible weaknesses of the assumptions adopted with the chosen mathematical models. The applied kinetic equations imply conditions, such as temperature distribution, liquid holdup, and mass transfer, which have to be measured in more detail to apply the model more correctly.

In general, the simulations based on the chosen model enable some new insights into the relationships in the studied CD. They allow to conduct qualitative and quasi-quantitative studies. The focus of the following studies is the CD column performance as a function of process parameters such as reboiler duty, residence time, and feed temperature, which are not directly connected with the hydrodynamic behavior of the CD column and therefore less affected by the simplified kinetics. The good agreement of simulated and experimental values of the DoDH at a feed rate of 0.2 g min⁻¹ suggests that this scenario can be taken as foundation for the base case for the following sensitivity analyses.

3.5. Parameter Analysis with the CD Simulation

To understand the CD process, sensitivity studies with variation of intensive independent parameters are carried out. Such quasi-quantitative analyses can give important insights to improve the performance of the column by tuning those process parameters. The EO simulation method was applied to optimize computation time. Starting with a converged CD simulation from a SM simulation, the EO method is very efficient for conducting simulations with a slight change of inputs. For sensitivity analyses, only an incremental change is imposed on the independent variable in each scenario. Hereby, the EO method converges to a new solution in only a few seconds.

As starting point for the sensitivity studies, a base case is defined. The DoDH of H12–BT dehydrogenation is targeted to be over 80% for an economical system of hydrogen storage and transport with LOHC.^[97] Therefore, the validated simulation at 0.2 g min⁻¹ is a good starting point. Also, here the relative error of the productivity of the simulation is only 5% when compared with the experiment. The process specifications of the experiment are converted to intensive quantities to generalize the subsequent analysis results. Slight modifications are made in the simulation for a better control. Details of the input parameters are listed in Table 1.

The simulation of the base case results in a CD performance with an overall DoDH of 71%. Full hydrogen release (DoDH = 100%) is avoided for the base case because in this case the sensitivity to the process parameters becomes marginal. At the top of the simulated CD column, the stream of the released

Table 1. Simulation specifications of the base case for the sensitivity analysis.

Simulation process parameter	Specifications and conditions
Mass-based residence time t^*/s^{-1}	9000
Catalyst weight/g	120
Feed rate $\dot{m}_{H_{12}-BT}/g \text{ min}^{-1}$	0.8
Boil-up ratio BR/–	14
Feed preheater duty/W	0
Column pressure/mbar	1013
Number of catalytic stages	3
Pressure drop per catalytic stage $\Delta p_{cat}/\text{mbar}$	0.36
Number of stripping stages	10
Pressure drop per stripping stage $\Delta p_{strip}/\text{mbar}$	2.1

hydrogen has a volumetric flow rate of 392 Nml min^{-1} and a purity of 99.99 mol%. The reflux stream at the top of the distillation section is much larger than the feed stream, which indicates a strong reflux in the CD column at $BR = 14$. When comparing the liquid flow at the top of the separation section with the liquid flow at the top of the catalytic section, it is clear that strong vapor condensation takes place in the catalytic section due to the fast endothermic reaction. According to the overall mass balance, only a small fraction of introduced mass flow leaves the process through the top stream which is mostly hydrogen. This is expected since a maximum of 6.2 wt% of the feed can be released as incondensable hydrogen gas. The rest is converted $H_x\text{-BT}$, which, whether dehydrogenated or not, is condensable and must leave the column via the bottom stream.

In the CD, many variables are dependent on each other due to the boiling condition. The pressure determines the temperature of the process and the CD is very sensitive to it because it affects the reaction equilibrium and the reaction rate.^[96] For the sensitivity studies, we consider operation at ambient pressure. Under these conditions, there are few degrees of freedom that are significant for the determination of the column's performance which include feed composition and temperature. Here, we want to focus on the mass-based residence time t^* and the BR. The influence of catalyst weight and feed rate on the CD performance can be viewed as equivalent. Therefore, t^* is defined as the ratio of the variable feed flow rate to the fixed catalyst amount and so becomes intensive. The reboiler duty is set in the experiment by adjusting \dot{V}_{evap} . For the simulation, the intensive parameter BR is selected inspired by the distillation literature. BR results from a material balance around the reboiler similar to the reflux ratio which emerges from balances around the condenser at the column top.^[56] Through the equilibrium stage assumption and omission of hydrodynamics in the column, the main performance indicators DoDH and productivity P are determined predominantly by t^* and BR. Both t^* and BR are defined intensively to make the subsequent results independent of the scale of the CD process (Equation (3) and (4))

$$t^* [s] = \frac{m_{\text{cat}}}{\dot{m}_{H_{12}-BT}} \quad (3)$$

$$BR = \frac{\dot{V}'}{B} \quad (4)$$

m_{cat} is the amount of catalyst in the CD column and $\dot{m}_{H_{12}-BT}$ is the feed flow rate of the reactant $H_{12}\text{-BT}$ that is introduced into the CD setup. \dot{V}' is the vapor mole flow rate from the bottom stage and B is the bottoms mole flow rate that is continuously removed from the CD setup.

Figure 7 depicts the sensitivity of DoDH and P to t^* . As expected, a higher residence time results in higher DoDH. The same positive effect on DoDH could be achieved by adding more catalyst to the setup or by using a more active catalyst. At high $t^* = 20\,000 \text{ s}$, almost all the chemically bound hydrogen has been released (DoDH > 97%). At higher t^* , the productivity decreases, because, on average, there is lower reactant concentration in the catalytic section.

Figure 8 shows that both DoDH and productivity improve with an increasing BR. A higher BR means that distillation is improved, and more vapor is available for a better heating of the reaction, so that the DoDH and hydrogen production per catalyst mass are increased. Regarding BR, two extreme scenarios are identified in the CD. For $BR < 5$, the simulation shows that the temperature in the catalyst section drops below 120°C . Insufficient heat supply brings the catalytic reaction almost to a standstill due to its own endothermic nature. The endothermic reaction is self-limiting due to the adiabatic model presumption. At a very low BR, the vapor phase is completely condensed before it reaches the top of the catalyst bed. The temperature on the catalytic stages is not high enough for effective hydrogen release. The top of the catalyst bed is simply too cold for dehydrogenation. The only outlet for the unconverted $H_{12}\text{-BT}$ is then the bottom stream. Therefore, the separation section is rather ineffective. At higher BRs, the large vapor stream can transfer more heat from the evaporator, which is the only heat source of the process, to the catalytic section. The BR depicts the idea how many times a molecule is evaporated internally before it leaves the column. The vapor condensation at the catalyst can then compensate

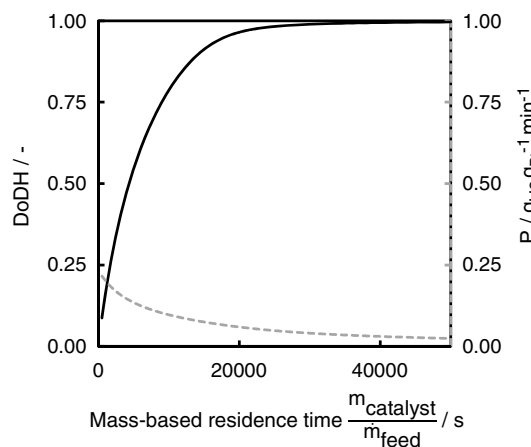


Figure 7. Sensitivity of performance indicators against varied mass-based residence time $t^* = m_{\text{cat}}/\dot{m}_{H_{12}-BT}$ at boil-up ratio $BR = 14$, $T_{\text{Feed}} = 30^\circ\text{C}$, $p = 1013 \text{ mbar}$, 3 CSTRs as catalytic stages + 10 non-catalytic stages + reboiler.

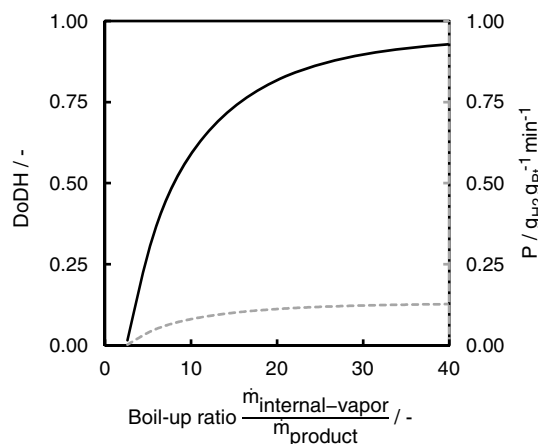


Figure 8. Sensitivity of performance indicators against varied boil-up ratio $BR = \dot{V}_{N_2} / \dot{B}$ at $t^* = 9000$ s, $T_{Feed} = 30$ °C, $p = 1013$ mbar, 3 CSTRs as catalytic stages + 10 non-catalytic stages + reboiler.

the endothermic dehydrogenation and maintains the temperature of the catalyst bed. To reach the goal of an overall H12–BT conversion of DoDH = 80%, the BR should be at least 18.8 at the given catalyst amount according to our model. However, the energy demand of the system increases with a higher BR. The reboiler duty is almost linearly correlated with BR. Since the heat demand of the column increases with higher BR, low BR are preferred for energetic reasons unless heat from an external heat source is available. As a result, there are two conflicting goals for the optimization of a CD with high DoDH: lower operating costs can be achieved by reducing the reboiler duty, but this has to be compensated by higher investment cost for a higher amount of catalyst and a larger reactor size. The trade-off between heat input and DoDH is very relevant to select suitable operation points for the hydrogen release from H12–BT by CD.

3.6. Heat Integration between CD and HT-PEM Operation

Finally, the CD process is analyzed with the focus on energy efficiency and heat management. Since hydrogen is often released from LOHC for power generation, the electric energy requirement of the CD process is highly relevant. To release hydrogen from H12–BT, it is necessary to break chemical bonds in the endothermic dehydrogenation reaction. The maximum theoretical energy yield of the LOHC-bound hydrogen-to-electricity can thus not exceed 74%. Thermodynamically 26% of the lower heating value (LHV) of the released hydrogen is required as reaction enthalpy at reaction temperature. Interestingly, the downstream hydrogen utilization steps, for example, hydrogen electrification in a fuel cell have efficiencies around 50% (based on the LHV of the used hydrogen) and can, therefore, serve as heat source for the hydrogen release step if their temperature level is high enough.^[28] By coupling the endothermic dehydrogenation with the off-gas heating from a high-temperature fuel cell, the efficiency from LOHC-bound hydrogen to electricity can be increased from 29 to 48%.^[98] This is also where CD offers huge potential as the CD process enables lowering of the LOHC

dehydrogenation temperature.^[28] It has been proposed some years ago to use solid oxide fuel cell (SOFC) waste heat as heat source for LOHC dehydrogenation^[31] and the technological potential of this coupling has been demonstrated^[32] resulting in a maximum efficiency of LOHC-bound hydrogen-to-electricity of 45%.^[33] Also, high-temperature PEM-FCs have been proposed as heat source for this combination.^[35–37] Note, however, that CD requires additional heat in addition to the reaction enthalpy for driving the distillation process. This extra heat is partly required for the thermodynamic enthalpy of demixing in the separation section and most of it is ejected as heat of lower temperature in the condenser at the top of the CD column.

In the following, we use the established CD simulation to investigate the viability of energetic coupling of fuel cell and CD. For this purpose, some further assumptions are made: electrical efficiencies of fuel cells are in the range of 40–60%^[30] and we assume 50%. Therefore, also the overall LOHC-bound hydrogen-to-electricity efficiency cannot exceed 50%. The heat demand of the reboiler is the only energy input to the CD setup. Feed preheating and the reaction enthalpy in the catalytic section are provided internally solely by condensing steam originating from the reboiler (Figure 9). Pumping is not considered and the condenser works with an energetically irrelevant coolant.^[99] Some heat leaves the system via the warm hydrogen and bottom streams. The column is assumed to be adiabatic for this simulation study to assess the mere viability of heat integration with a hydrogen-consuming fuel cell. Heat losses are difficult to quantify in an experimental setup and would not match conditions after scale-up. Adiabatic operation is also a viable approximation if the setup is scaled-up as in the case of industrial distillation columns.^[100] The decisive question is now whether the heat demand of the reboiler can be lower than the waste heat of the fuel cell. To indicate this, the heat availability (HA) is defined in Equation (5). Since HA is obtained purely based on the energy balance, the temperature profiles of the heat exchange are not considered. When $HA > 100\%$, the reboiler can be sufficiently heated by the fuel cell off-gas alone. Otherwise, auxiliary heating might be necessary to support the CD process.

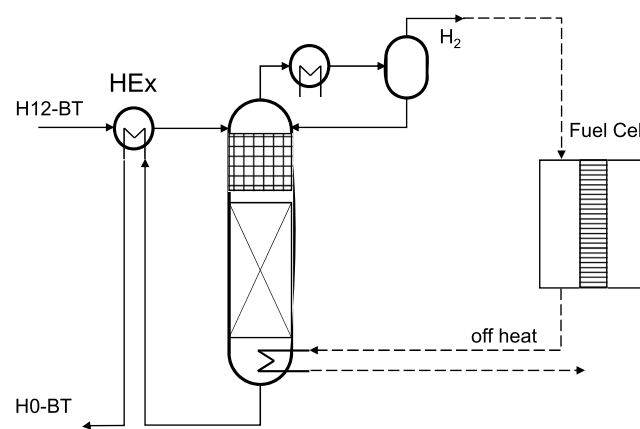


Figure 9. Flow sheet of the coupled CD column and the fuel cell with feed-product heat exchange for the CD.

$$HA = \frac{0.5 \cdot LHV_{H_2}}{\dot{Q}_{rb}} \quad (5)$$

The results of thermal coupling between CD and fuel cell are depicted in **Figure 10**. The graphs show the relationship between the available fuel cell waste heat and the heat demand of the reboiler. As depicted in Figure 10, for the base case, with no heat exchanger (NoHEX, cf. Table 1), only BR values close to the optimal BR of 6.8 can enable an autothermic operation through the coupling of fuel cell and CD. At higher BR, the catalytic and the separation section work well, and the fuel cell consumes hydrogen and produces off-heat, which, however, is not enough since too much heat is lost via the condenser. At lower BR, not enough heat is supplied to the reaction section and the dehydrogenation comes to a standstill. Heating up feed and catalytic section consume all the heat whereas hardly any hydrogen is released that can be consumed by the fuel cell to produce any off-heat there. Under these circumstances, a major part of the reboiler duty is used to heat up the cold feed stream. In such a simple setup without heat recovery, the liquid flow that has passed the column leaves the process as bottom stream at high temperature. This part of sensible heat is wasted without heat recovery.

To utilize the heat lost through the bottom product stream, a heat exchanger between feed and bottom streams is introduced (HEX in Figure 9). Up to 14% of the reboiler duty can be recovered through such a heat exchanger. This boosts the temperature in the catalytic section and ultimately the dehydrogenation rate of H12-BT. The maximum HA shifts to lower BR and the possible BR range for a fully heat-integrated process becomes much wider. BR should then be in the range of $2.8 \leq BR \leq 9.4$ and correspondingly, the maximal DoDH of H12-BT in this range is 60%. This shows that process parameters allowing full heat integration are in the range of technical relevance.

Further optimization measures are the adding of more stripping stages for better separation, the vapor recompression

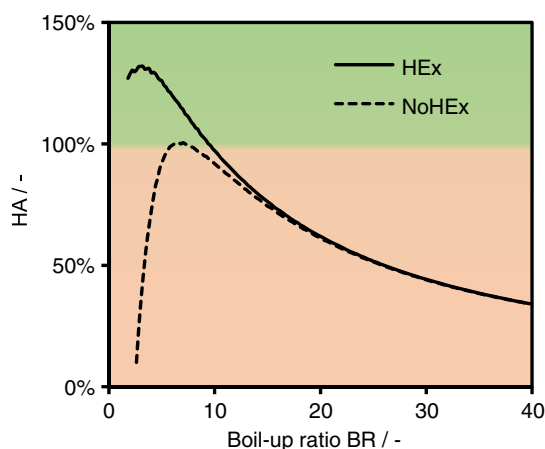


Figure 10. Heat integration potentials between CD and high-temperature PEM (HT-PEM) fuel cell operation; dashed line: base case CD column; solid line: CD column with feed/product heat exchanger and heat coupling of reboiler and fuel cell exhaust gas; electrical efficiency of the fuel cell is assumed to be 50% (based on the LHV of hydrogen), and the feasible and infeasible thermal coupling of the CD reboiler with the fuel cell are represented by the green and orange areas, respectively.

before the condenser to upgrade the heat here and the adding of separation stages at the column top to act as pre-condenser and heat buffer zone for the reflux. The latter would prevent direct contact of the cold reflux (40 °C) from the condenser with the catalyst pellets in the top of the catalytic section. Nonetheless, the most important improvement lies in the development of better dehydrogenation catalysts. Higher catalytic activity^[10,11,101] and an optimized catalyst shape^[102–105] can further increase the effectiveness of the hydrogen release by CD at BRs where a fully heat-integrated process is viable.

4. Conclusion

We have investigated the performance of the steady-state continuous dehydrogenation of H12-BT through CD. At first, an increased hydrogen release rate was demonstrated when employing a separation section. This is due to the fact that the concentration of H12-BT is enriched toward the column top where the catalyst section is placed. In addition, the negative influence of product inhibition on the catalyst is reduced if the separation section is applied. In a direct comparison with a conventional liquid-phase dehydrogenation of H18-DBT, the CD of H12-BT achieves up to sixfold higher hydrogen release rate at the same temperature level, which is clearly beyond the reactivity difference of both reactants. At the mild temperature of 267 °C, the H12-BT dehydrogenation via CD featured a remarkable platinum-based productivity of $0.35 \text{ g}_{H_2} \text{ g}_{Pt}^{-1} \text{ min}^{-1}$ ($0.7 \text{ kW g}_{Pt}^{-1}$) at a conversion of DoDH = 30%. Runs with half the catalyst amount in the CD setup exhibited the same Pt-based productivity, and stable countercurrent flow conditions occurred in the CD column. Stable operation of the CD process was realized in the applied experimental setup for several hours of time-on-stream.

Further, we simulated the CD process based on experimentally founded models to identify potentials to improve the process design. In the base case simulation, 71% of the stored hydrogen are released (DoDH = 71%) at a mass-based residence time $t^* = m_{cat}/\dot{m}_F = 6000 \text{ s}$ and a $BR = \dot{V}/\dot{B} = 14$. The sensitivity analysis shows that t^* can improve the DoDH in H12-BT dehydrogenation. However, the productivity P decreases as t^* increases. When t^* is $>20\,000 \text{ s}$ and DoDH is $>96\%$, the addition of more catalyst becomes ineffective. The variation of BR reveals that both DoDH and productivity rise with an increasing BR. The goal of 80% DoDH is reached at $BR > 18.8$. Two conflicting goals are identified for achieving high DoDHs: On the one hand, low operating costs call for low BR to reduce heat consumption. On the other hand, low BR requires larger masses of catalyst and a larger dehydrogenation setup to reach high DoDHs, which increases investment cost. An alternative way of system optimization is the development of more active dehydrogenation catalysts, in particular for the temperature range below 270 °C.

Finally, the heat integration between a HT-PEM hydrogen fuel cell and the CD has been studied from an HA point of view. By applying an additional heat exchanger to recuperate heat from the hot product LOHC stream, the fuel cell waste heat can fully provide the total heat demand of the CD over an expedient range of BRs and no external heat source is required. This paves the way for fully heat-integrated combinations of LOHC dehydrogenation via CD and hydrogen electrification in HT-PEM systems.

Supporting Information

Supporting Information is available from the Wiley Online Library or from the author.

Acknowledgements

The authors acknowledge financial support by the BMBF through the cluster B1 of the Kopernikus “Power2X” project. In addition, the authors gratefully acknowledge infrastructural support by the Bavarian Ministry of Economic Affairs, Regional Development and Energy, and the “Energie Campus Nürnberg.” Furthermore, this work was funded by the Bavarian Ministry of Economic Affairs, Regional Development and Energy through the project “Emissionsfreier und stark emissionsreduzierter Bahnverkehr auf nicht-elektrifizierten Strecken.”

Open Access funding enabled and organized by Projekt DEAL.

Conflict of Interest

The authors declare no conflict of interest.

Data Availability Statement

The data that support the findings of this study are available from the corresponding author upon reasonable request.

Keywords

catalytic distillation, continuous dehydrogenation, heat integration, hydrogen storage, perhydro benzyltoluene

Received: November 21, 2022

Revised: December 15, 2022

Published online:

- [1] D. Teichmann, W. Arlt, P. Wasserscheid, R. Freymann, *Energy Environ. Sci.* **2011**, *4*, 2767.
- [2] P. T. Aakko-Saksa, C. Cook, J. Kiviaho, T. Repo, *J. Power Sources* **2018**, *396*, 803.
- [3] P. Preuster, C. Papp, P. Wasserscheid, *Acc. Chem. Res.* **2017**, *50*, 74.
- [4] D. Teichmann, W. Arlt, P. Wasserscheid, *Int. J. Hydrogen Energy* **2012**, *37*, 18118.
- [5] K. Müller, K. Stark, V. N. Emel'yanenko, M. A. Varfolomeev, D. H. Zaitsau, E. Shoifet, C. Schick, S. P. Verevkin, W. Arlt, *Ind. Eng. Chem. Res.* **2015**, *54*, 7967.
- [6] C. Krieger, *Dissertation*, Friedrich-Alexander-Universität Erlangen-Nürnberg (FAU), (Erlangen) **2019**.
- [7] T. Rüde, S. Dürr, P. Preuster, M. Wolf, P. Wasserscheid, *Sustainable Energy Fuels* **2022**, *6*, 1541.
- [8] Y. Kwak, J. Kirk, S. Moon, T. Ohm, Y.-J. Lee, M. Jang, L.-H. Park, C.-I. Ahn, H. Jeong, H. Sohn, S. W. Nam, C. W. Yoon, Y. S. Jo, Y. Kim, *Energy Convers. Manage.* **2021**, *239*, 114124.
- [9] F. Auer, D. Blaumeiser, T. Bauer, A. Bösmann, N. Szesni, J. Libuda, P. Wasserscheid, *Catal. Sci. Technol.* **2019**, *9*, 3537.
- [10] F. Auer, A. Hupfer, A. Bösmann, N. Szesni, P. Wasserscheid, *Catal. Sci. Technol.* **2020**, *10*, 6669.
- [11] N. Szesni, F. Frankl, S. Sturm, P. Wasserscheid, A. Seidel, A. Boesmann, (Clariant International Ltd), *Ger. DE102018109254A1*, **2019**.
- [12] H. Jorschick, M. Geißelbrecht, M. Eßl, P. Preuster, A. Bösmann, P. Wasserscheid, *Int. J. Hydrogen Energy* **2020**, *29*, 14897.
- [13] T. W. Kim, S. Park, J. Oh, C. H. Shin, Y. W. Suh, *ChemCatChem* **2018**, *10*, 3406.
- [14] T. W. Kim, C. Kim, H. Jeong, C.-H. Shin, Y.-W. Suh, *Korean J. Chem. Eng.* **2020**, *37*, 1427.
- [15] N. Brückner, K. Obesser, A. Bösmann, D. Teichmann, W. Arlt, J. Dungs, P. Wasserscheid, *ChemSusChem* **2014**, *7*, 229.
- [16] P. Runge, C. Sölch, J. Albert, P. Wasserscheid, G. Zöttl, V. Grimm, <https://ssrn.com/abstract=3623514> (accessed: July 2020).
- [17] M. Niermann, S. Drünert, M. Kaltschmitt, K. Bonhoff, *Energy Environ. Sci.* **2019**, *12*, 290.
- [18] Y. Okada, M. Shimura, presented at *Technical paper at Joint GCC-JAPAN Environment Symp.*, Japan **2013**.
- [19] Y. Okada, K. Imagawa, M. Yasuic, <https://www.shokubai.org/tocat8/pdf/Plenary/PL9.pdf> (accessed: November 2022).
- [20] E. Newson, T. Haueter, P. Hottinger, F. Von Roth, G. Scherer, T. H. Schucan, *Int. J. Hydrogen Energy* **1998**, *23*, 905.
- [21] M. S. Akram, M. R. Usman, *Theor. Found. Chem. Eng.* **2021**, *55*, 545.
- [22] L. Wagner, *Dissertation*, Friedrich-Alexander-Universität Erlangen-Nürnberg (FAU), (Erlangen) **2020**.
- [23] A. Fikrt, R. Brehmer, V.-O. Milella, K. Müller, A. Bösmann, P. Preuster, N. Alt, E. Schlücker, P. Wasserscheid, W. Arlt, *Appl. Energy* **2017**, *194*, 1.
- [24] J. Geiling, M. Steinberger, F. Ortner, R. Seyfried, A. Nuß, F. Uhrig, C. Lange, R. Öchsner, P. Wasserscheid, M. März, P. Preuster, *Int. J. Hydrogen Energy* **2021**, *46*, 35662.
- [25] N. Heublein, M. Stelzner, T. Sattelmayer, *Int. J. Hydrogen Energy* **2020**, *45*, 24902.
- [26] H. Jorschick, P. Preuster, S. Dürr, A. Seidel, K. Müller, A. Bösmann, P. Wasserscheid, *Energy Environ. Sci.* **2017**, *10*, 1652.
- [27] H. Jorschick, S. Dürr, P. Preuster, A. Bösmann, P. Wasserscheid, *Energy Technol.* **2019**, *7*, 146.
- [28] K. Müller, T. Skeledzic, P. Wasserscheid, *Energy Fuels* **2021**, *35*, 10929.
- [29] K. Knosala, L. Kotzur, F. T. C. Röben, P. Stenzel, L. Blum, M. Robinius, D. Stolten, *Int. J. Hydrogen Energy* **2021**, *46*, 21748.
- [30] R. O'Hayre, S.-W. Cha, W. Colella, F. B. Prinz, *Fuel Cell Fundamentals*, John Wiley & Sons, Hoboken, NJ **2016**.
- [31] M. Ichikawa, in *Solid-State Hydrogen Storage*, Vol. 1 (Ed: G. Walker), Woodhead Publishing, Sawston, Cambridge **2008**, p. 500.
- [32] P. Preuster, Q. Fang, R. Peters, R. Deja, V. N. Nguyen, L. Blum, D. Stolten, P. Wasserscheid, *Int. J. Hydrogen Energy* **2018**, *43*, 1758.
- [33] R. Peters, R. Deja, Q. Fang, V. N. Nguyen, P. Preuster, L. Blum, P. Wasserscheid, D. Stolten, *Int. J. Hydrogen Energy* **2019**, *44*, 13794.
- [34] D. Stolten, B. Emonts, *Fuel Cell Science and Engineering: Materials, Processes, Systems and Technology*, John Wiley & Sons, Weinheim **2012**.
- [35] K.-S. Lee, S. Maurya, Y. S. Kim, C. R. Kreller, M. S. Wilson, D. Larsen, S. E. Elangovan, R. Mukundan, *Energy Environ. Sci.* **2018**, *11*, 979.
- [36] G. Venugopalan, K. Chang, J. Nijoka, S. Livingston, G. M. Geise, C. G. Arges, *ACS Appl. Energy Mater.* **2020**, *3*, 573.
- [37] M. Geißelbrecht, S. Mrusek, K. Müller, P. Preuster, A. Bösmann, P. Wasserscheid, *Energy Environ. Sci.* **2020**, *13*, 3119.
- [38] G. J. Harmsen, *Chem. Eng. Process. Process Intensif.* **2007**, *46*, 774.
- [39] A. Kołodziej, M. Jaroszyński, A. Hoffmann, A. Górak, *Catal. Today* **2001**, *69*, 75.
- [40] M. Sakuth, D. Reusch, R. Janowsky, in *Ullmann's Encyclopedia of Industrial Chemistry*, Wiley-VCH, Weinheim **2008**.
- [41] A. Gaurav, *Dissertation*, University of Waterloo, (Waterloo, Ontario, Canada) **2017**.
- [42] A. A. Kiss, *Advanced Distillation Technologies: Design, Control and Applications*, John Wiley & Sons, Chichester **2013**.
- [43] G. Podrebarac, F. T. Ng, G. Rempel, *Chem. Tech.* **1997**, *27*, 37.

- [44] P.-A. D. Gaspillo, L. C. Abella, S. Goto, *J. Chem. Eng. Jpn.* **1998**, *31*, 440.
- [45] A. Heintz, *Thermodynamik: Grundlagen und Anwendungen*, 2nd ed., Springer Spektrum, Berlin **2017**.
- [46] U. Onken, W. Arlt, *Recommended Test Mixtures for Distillation Columns*, 2nd ed., Institution of Chemical Engineers, Rugby, Warwickshire, England **1990**.
- [47] C. R. Ortiz, F. Dolci, R. E. Weidner, *Assessment of Hydrogen Delivery Options: Feasibility of Transport of Green Hydrogen Within Europe*, Publications Office of the European Union, Luxembourg, **2022**.
- [48] M. Doherty, Z. Fidkowski, M. Malone, R. Taylor, *Perry's Chemical Engineers' Handbook*, 8th ed., McGraw-Hill, New York **2007**.
- [49] K. Sattler, *Thermische Trennverfahren: Grundlagen, Auslegung, Apparate*, 3rd ed., Wiley-VCH, Weinheim **2001**.
- [50] E. Krell, *Handbook of Laboratory Distillation*, Elsevier, Amsterdam, Oxford, New York **1982**.
- [51] M. Geißelbrecht, *Dissertation*, Friedrich-Alexander-Universität Erlangen-Nürnberg (FAU), (Erlangen) **2020**.
- [52] Clariant-International-Ltd, <https://www.clariant.com/en/Solutions/Products/2019/05/21/15/19/Elemax-Series> (accessed: November 2021).
- [53] T. Keller, in *Distillation* (Eds: A. Górac, Ž. Olujić), Academic Press, Boston **2014**, pp. 261.
- [54] J. Ellenberger, R. Krishna, *Chem. Eng. Sci.* **1999**, *54*, 1339.
- [55] R. Taylor, R. Krishna, *Chem. Eng. Sci.* **2000**, *55*, 5183.
- [56] R. Goedecke, *Fluidverfahrenstechnik: Grundlagen, Methodik, Technik, Praxis*, Wiley-VCH, Weinheim **2006**.
- [57] R. Baur, A. Higler, R. Taylor, R. Krishna, *Chem. Eng. J.* **2000**, *76*, 33.
- [58] K. A. I. Sundmacher, L. K. Rihko, U. Hoffmann, *Chem. Eng. Commun.* **1994**, *127*, 151.
- [59] J. D. Seader, E. J. Henley, D. K. Roper, *Separation Process Principles*, 3rd ed., John Wiley, Hoboken, New Jersey **2010**.
- [60] K. Sundmacher, U. Hoffmann, *Chem. Eng. Sci.* **1994**, *49*, 3077.
- [61] A. Fredenslund, *Vapor-Liquid Equilibria using UNIFAC: A Group-Contribution Method*, Elsevier, Amsterdam, Oxford, New York **1977**.
- [62] U. Weidlich, *Dissertation*, TU Dortmund University, (Dortmund) **1985**.
- [63] U. Weidlich, J. Gmehling, *Ind. Eng. Chem. Res.* **1987**, *26*, 1372.
- [64] A. Jakob, H. Grensemann, J. Lohmann, J. Gmehling, *Ind. Eng. Chem. Res.* **2006**, *45*, 7924.
- [65] J. Gmehling, J. Lohmann, A. Jakob, J. Li, R. Joh, *Ind. Eng. Chem. Res.* **1998**, *37*, 4876.
- [66] DDBST-GmbH, <http://unifac.ddbst.de/unifacga.html> (accessed: April 2022).
- [67] A. Jess, P. Wasserscheid, *Chemical Technology: From Principles to Products*, Wiley-VCH, Weinheim **2020**.
- [68] O. Levenspiel, *Chemical Reaction Engineering*, 3rd ed., Wiley, NY **1999**.
- [69] T. Oehmichen, *Dissertation*, Universität Bayreuth, (Bayreuth) **2011**.
- [70] L. B. Datsevich, *Appl. Catal., A* **2005**, *294*, 22.
- [71] T. Solymosi, M. Geißelbrecht, S. Mayer, M. Auer, P. Leicht, M. Terlinden, P. Margaretti, A. Bösmann, P. Preuster, J. Harting, M. Thommes, N. Vogel, P. Wasserscheid, *Sci. Adv.* **2022**, *8*, eade3262.
- [72] J. Maćkowiak, *Fluiddynamik von Füllkörpern und Packungen*, Springer, Berlin, Heidelberg **2003**.
- [73] S. Schug, *Dissertation*, Friedrich-Alexander-Universität Erlangen-Nürnberg (FAU), (Erlangen) **2018**.
- [74] A. Tuchlenski, A. Beckmann, D. Reusch, R. Düssel, U. Weidlich, R. Janowsky, *Chem. Eng. Sci.* **2001**, *56*, 387.
- [75] W. Reschetilowski, *Handbuch Chemische Reaktoren*, Springer, Berlin **2021**.
- [76] J.-L. Kang, Y.-C. Ciou, D.-Y. Lin, D. S.-H. Wong, S.-S. Jang, *Chem. Eng. Res. Des.* **2019**, *147*, 43.
- [77] Y. Haroun, L. Raynal, D. Legendre, *Chem. Eng. Sci.* **2012**, *75*, 342.
- [78] P. Preuster, *Dissertation*, Friedrich-Alexander-Universität Erlangen-Nürnberg (FAU), (Erlangen) **2017**.
- [79] A. Seidel, *Dissertation*, Friedrich-Alexander-Universität Erlangen-Nürnberg (FAU), (Erlangen) **2019**.
- [80] S. Mrusek, *Dissertation*, Friedrich-Alexander-Universität Erlangen-Nürnberg (FAU), (Erlangen) **2022**.
- [81] P. Virtanen, R. Gommers, T. E. Oliphant, M. Haberland, T. Reddy, D. Cournapeau, E. Burovski, P. Peterson, W. Weckesser, J. Bright, *Nat. Methods* **2020**, *17*, 261.
- [82] Sasol-Performance-Chemicals, https://www.sasolgermany.de/fileadmin/doc/alumina/Neu_2017/SasoL_Shaped_Carriers_Flyer_07_08_17_23-00_Webversion_Einzelseiten.pdf (accessed: October 2022).
- [83] Merck-KGaA, <https://www.sigmaaldrich.com/DE/en/sds/ALDRICH/172456> (accessed: December 2022).
- [84] Merck-KGaA, https://www.merckmillipore.com/DE/de/product/msds/MDA_CHEM-820633?Origin=PDP (accessed: December 2022).
- [85] A. Kołodziej, M. Jaroszyński, H. Schoenmakers, K. Althaus, E. Geißler, C. Übler, M. Kloeker, *Chem. Eng. Process. Process Intensif.* **2005**, *44*, 661.
- [86] A. Gorak, M. Jaroszyński, A. Kołodziej, *Chem. Pap.* **2006**, *60*, 404.
- [87] H. Ding, W. Xiang, N. Song, C. Liu, X. Yuan, *Chem. Eng. Technol.* **2014**, *37*, 1127.
- [88] J. Gmehling, M. Kleiber, B. Kolbe, J. Rarey, *Chemical Thermodynamics for Process Simulation*, Wiley-VCH, Weinheim **2019**.
- [89] K. Müller, R. Aslam, A. Fischer, K. Stark, P. Wasserscheid, W. Arlt, *Int. J. Hydrogen Energy* **2016**, *41*, 22097.
- [90] A. Leinweber, K. Müller, *Energy Technol.* **2018**, *6*, 513.
- [91] R. Aslam, *Dissertation*, Friedrich-Alexander-Universität Erlangen-Nürnberg (FAU), (Erlangen) **2016**.
- [92] T. Solymosi, F. Auer, S. Dürr, P. Preuster, P. Wasserscheid, *Int. J. Hydrogen Energy* **2021**, *46*, 34797.
- [93] M. Guisnet, P. Magnoux, in *Studies in Surface Science and Catalysis*, Vol. 88 (Eds: B. Delmon, G. F. Froment), Elsevier, Amsterdam, Lausanne, New York, Oxford, Shannon, Tokyo **1994**, p. 53.
- [94] K. Sundmacher, A. Kienle, *Reactive Distillation: Status and Future Directions*, Wiley-VCH, Weinheim **2003**.
- [95] L. T. Biegler, I. E. Grossmann, A. W. Westerberg, *Systematic Methods for Chemical Process Design*, Prentice Hall, NJ **1997**.
- [96] A. W. Dowling, L. T. Biegler, *Comput. Chem. Eng.* **2015**, *72*, 3.
- [97] S. Mrusek, P. Preuster, K. Müller, A. Bösmann, P. Wasserscheid, *Int. J. Hydrogen Energy* **2021**, *46*, 15624.
- [98] K. Müller, S. Thiele, P. Wasserscheid, *Energy Fuels* **2019**, *33*, 10324.
- [99] Gas-Processors-Suppliers-Association, *Engineering Data Book*, 12th ed., Gas Processors Suppliers Association (GPSA), Tulsa, Oklahoma **2004**.
- [100] K. Sattler, T. Adrian, *Thermische Trennverfahren: Aufgaben und Auslegungsbeispiele*, 2nd ed., Wiley VCH, Weinheim **2016**.
- [101] Y. Sekine, T. Higo, *Top. Catal.* **2021**, *64*, 470.
- [102] F. Schüth, M. Hesse, in *Handbook of Heterogeneous Catalysis*, Wiley-VCH, Weinheim **2008**, p. 676.
- [103] N. Katashani-Shirazi, V. Wloka, W. Gerlinger, A. Schmidt, K. Heinen, W. Kollenberg, (BASF SE), *Ger. WO2009047141A1*, **2009**.
- [104] K. Gottlieb, W. Graf, K. Schadlich, U. Hoffmann, A. Rehfinger, J. Flato, (Veba Oel AG), USA, *US005244929A*, **1993**.
- [105] G. Prieto, F. Schüth, *Angew. Chem. Int. Ed.* **2015**, *54*, 3222.
- [106] H. Z. Kister, J. R. Haas, D. R. Hart, D. R. Gill, *Distillation Design*, Vol. 1, McGraw-Hill, New York **1992**.